The phenoxides react with 4 molar equiv of methyllithium to give the tetraalkyls, $Me_4M(dmpe)_2$, where M is Th or U. Both phenoxides crystallize from toluene as toluene solvates $(PhO)_4M(dmpe)_2{\cdot}C_7H_8$ (M = U,[12] M = Th[13]).

Since the uranium complexes may be converted into each other, in isolated yields of ≥85% (Scheme I), the crystal structure of any one of them proves the existence of all of them as authentic tertiary phosphine complexes of uranium. In addition, the infrared spectrum and powder X-ray diffraction pattern of $U(OPh)_4(dmpe)_2{\cdot}C_7H_8$ are identical with those of $Th(OPh)_4(dmpe)_2{\cdot}C_7H_8$. Thus, the thorium phenoxide is isostructural with its uranium analogue. Since the thorium derivatives may be converted into each other, they are also authentic phosphine complexes.

An ORTEP[14] diagram of $U(OPh)_4(dmpe)_2$ is shown in Figure 1, and a line drawing is shown in Figure 2 with some bond angles and lengths. The coordination polyhedron is related to that of a $D_{2d}$ dodecahedron with the four phosphorus atoms and the four oxygen atoms occupying the A and B sites, respectively.[15] The shape parameters will be discussed in a full paper. The average uranium–oxygen bond length of 2.17 ± 0.01 Å is in the range observed for other uranium alkoxide–oxygen bonds.[16] The average uranium–phosphorus bond length of 3.104 ± 0.006 Å is unique, so no direct comparison is possible, though an estimate can be made. The tetrahedral covalent radius of a phosphorus atom is 0.44 Å larger than that of an oxygen atom.[17] Hence a uranium–phosphorus bond length of 2.6 Å may be estimated, rather shorter than that observed. On the other hand, a value of 2.9–3.0 Å may be estimated from the eight-coordinate $MX_4(diars)_2$ complexes, where M is a group 4b or 5b metal, when the radii of arsenic and the transition metals are taken into account.[18] The latter estimated value is much closer to the value observed.

**Acknowledgment.** This work was supported by the Director, Office of Energy Research, Office of Basic Energy Sciences, Chemical Sciences Division of the U.S. Department of Energy, under Contract W-7405-ENG-48. We thank the NSF for an equipment grant to the Chemistry Department used for the purchase of the X-ray diffractometer. We thank Dr. F. L. Hollander, staff crystallographer of the U.C. Berkeley X-ray facility (CHEXRAY) for collecting the X-ray data.

**Note Added in Proof.** The preparation and crystal structure of $U(Me_5C_5)_2H(dmpe)$ was announced in a lecture by T. J. Marks at the 28th I.U.P.A.C. congress in Vancouver, B.C. (August 17–20, 1981).

**Supplementary Material Available:** Positional and thermal parameters and estimated standard deviations and estimated atomic parameters for the hydrogen atoms and anisotropic thermal parameters (3 pages). Ordering information is given on any current masthead page.

---

(12) Anal. Calcd for $C_{43}H_{60}O_4P_4U$: C, 51.5; H, 5.99; P, 12.4. Found: C, 51.3; H, 5.98; P, 12.2. $^1H$ NMR ($PhMe\text{-}d_8$, −24 °C): three resonances are attributable to the phenyl protons at $\delta$ 33.45, doublet ($J$ = 7.3 Hz), $\delta$ 15.59, binomial triplet ($J$ = 7.3 Hz), and $\delta$ 13.59, binomial triplet ($J$ = 7.3 Hz), in area ratio 8:8:4 due to ortho, meta, and para protons, respectively. The resonances due to dmpe occur as broad, apparent singlets at $\delta$ −3.78 ($Me_2P$) and $\delta$ −32.86 ($CH_2P$) ($\nu_{1/2}$ = 40 Hz in each case) in area ratio 24:8, respectively. Resonances due to toluene of crystallization appear at $\delta$ 7.04 (s) and $\delta$ 2.12 (s), due to the phenyl and methyl protons, in area ratio 5:3, respectively.

(13) Anal. Calcd for $C_{43}H_{60}O_4P_4Th$: C, 51.8; H, 6.02; P, 12.5. Found: C, 52.1; H, 5.98; P, 12.9. $^1H$ NMR ($PhMe\text{-}d_8$, 40 °C): the phenyl resonance appears on a broad ($\nu_{1/2}$ = 41 Hz) complex multiplet centered at $\delta$ 7.04 and includes the phenyl resonance of toluene of crystallization. The methyl protons of toluene give rise to a singlet ($\delta$ 2.14); dmpe methylene protons produce an apparent three-line pattern with the central line at $\delta$ 1.16 and the separation between the two outer lines being 12.2 Hz and a broad singlet, $\delta$ 0.82 ($\nu_{1/2}$ = 6 Hz, $Me_2P$). The resonances have relative area ratios 25:3:8:24. $^{13}C\{^1H\}$ NMR ($CD_2Cl_2$, −50 °C): the aromatic carbons give rise to four singlets at $\delta$ 167.44 ($\alpha$ to oxygen), 128.91 ($\beta$ to oxygen), 119.50 ($\gamma$ to oxygen), and 115.99 ($\delta$ to oxygen). Assignment is confirmed by the $^{13}C$ spectrum where the three high field signals are observed as doublets ($J_{C\text{-}H}$ = 148.4, 159.2, and 161.1 Hz, respectively) and the quaternary carbon ($\delta$ 167.44) remains as a singlet. Two broad singlets at $\delta$ 27.06 ($P\text{-}CH_2$, $\nu_{1/2}$ = 32 Hz) and $\delta$ 13.23 ($Me_2P$, $\nu_{1/2}$ = 35 Hz) are due to dmpe. $^{31}P\{^1H\}$ NMR ($PhMe\text{-}d_8$, −60 °C): $\delta$ −12.0. The coordination chemical shift is 30.2 ppm.

(14) The crystals are triclinic, $P\bar{1}$, with cell dimensions $a$ = 12.560 (4) Å, $b$ = 12.831 (4) Å, $c$ = 15.012 (4) Å, $\alpha$ = 77.84 (3)°, $\beta$ = 83.28 (3)°, and $\gamma$ = 88.94 (3)°. For two molecules in the unit cell the calculated density is 1.29 g/cm$^3$. Intensity data were collected with a Nonius CAD-4 automated X-ray diffractometer by using Mo K$\alpha$ X-rays. The structure was solved by the "heavy-atom" technique and refined by full-matrix least squares to an $R$ factor of 0.052 using 5090 reflections for which $F^2 > 3\sigma(F^2)$.

(15) Hoard, J. L.; Silverton, J. V. *Inorg. Chem.* **1963**, *2*, 235–243.

(16) (a) 2.237 ± 0.008 Å in tetrakis(hexafluoroacetonylpyrazolide)uranium(IV): Volz, K.; Zalkin, A.; Templeton, D. H. *Inorg. Chem.* **1976**, *15*, 1827–1831. (b) 2.375 ± 0.013 Å in the tetrakis(catecholato)uranate(IV): Sofen, S. R.; Abu-Dari, K.; Freyberg, D. P.; Raymond, K. N. *J. Am. Chem. Soc.* **1978**, *100*, 7882–7887. (c) 2.06 ± 0.01 Å in tetrakis(allyl)tetrakis(isopropoxo)diuranium(IV): Brunelli, M.; Perego, G.; Lugli, G.; Mazzei, A. *J. Chem. Soc., Dalton Trans.* **1979**, 861–868.

(17) Pauling, L. "The Nature of the Chemical Bond"; Cornell University Press: Ithaca, NY, **1960**; p 246.

(18) Kepert, D. L. *Prog. Inorg. Chem.* **1978**, *24*, 179–249.

---

# Kinetics of the Anaerobic Reduction of Ferricytochrome $cd_1$ by $Fe(EDTA)^{2-}$. Evidence for Bimolecular and Intramolecular Electron Transfers to the $d_1$ Hemes

Steven A. Schichman and Harry B. Gray*

*Contribution No. 6475*
*from the Arthur Amos Noyes Laboratory*
*California Institute of Technology*
*Pasadena, California 91125*

*Received July 6, 1981*

One of the major goals of bioinorganic chemistry is the elucidation of the pathways employed by metalloenzymes that are involved in multielectron oxidation–reduction catalytic reactions. Our recent work in this area has centered on *Pseudomonas aeruginosa* cytochrome $cd_1$ (ferrocytochrome $c_{551}$:oxygen oxidoreductase, EC 1.9.3.2), a water soluble enzyme in which spectroscopically distinct heme groups (one $c$ and one $d_1$) are contained in each of two identical 63 000-dalton subunits.[1-5] The enzyme is particularly well suited for detailed electron-transfer mechanistic investigations, because the oxidation levels of the two different hemes [$E(c^{3+/2+})$ = 0.294; $E(d_1{}^{3+/2+})$ = 0.287 V vs. NHE)[6] can be monitored readily by electronic absorption spectroscopy.

We have completed an investigation of the kinetics of anaerobic $Fe(EDTA)^{2-}$ reduction of ferricytochrome $cd_1$.[7] The reduction of the heme $c$ groups is monophasic, whereas biphasic kinetics are observed for electron transfer to the $d_1$ hemes. Pseudo-first-order rate constants for reduction of the $c$ hemes and those for the fast $d_1$ phase vary linearly with the concentration of $Fe(EDTA)^{2-}$; in contrast, the slow $d_1$ phase exhibits rate saturation (Figure 1). The amplitudes of the two phases of the heme $d_1$ reaction are approximately equal, and the absorbance vs. time curves reveal clearly defined induction periods.

---

(1) Kuronen, T.; Ellfolk, N. *Biochim. Biophys. Acta* **1972**, *275*, 308–318.

(2) Kuronen, T.; Saraste, M.; Ellfolk, N. *Biochim. Biophys. Acta* **1975**, *393*, 48–54.

(3) Silvestrini, M. C.; Colosimo, A.; Brunori, M.; Walsh, T. A.; Barber, D.; Greenwood, C. *Biochem. J.* **1979**, *183*, 701–709.

(4) Takano, T.; Dickerson, R. E.; Schichman, S. A.; Meyer, T. E. *J. Mol. Biol.* **1979**, *133*, 185–188.

(5) Schichman, S. A. Ph.D. Thesis University of Chicago, 1981.

(6) Midpoint potentials were determined by thin-layer spectroelectrochemical methods (Taniguchi, V. T.; Sailasuta-Scott, N.; Anson, F. C.; Gray, H. B. *Pure Appl. Chem.* **1980**, *52*, 2275–2281) from plots of $E$(applied) vs. log ([O]/[R]) for the $c$ (548 nm; 40 (2) mV slope) and $d_1$ (670 nm; 33 (2) mV slope) hemes. Conditions: 25 °C; pH 7.0, $\mu$ = 0.1 M (sodium phosphate); mediator $[Ru(NH_3)_5py](ClO_4)_3$ (Taniguchi, V. T.; Schichman, S. A.; Ellis, W. R., Jr.; Cammarata, V.; Gray, H. B., to be submitted for publication).

(7) The enzyme was purified from bacterial paste by a modification[5] of a standard procedure.[1] Crystalline material[4] was used in all experiments. Stopped-flow kinetic measurements under anaerobic conditions and data analyses were performed as described previously (Scott, R. A.; Gray, H. B. *J. Am. Chem. Soc.* **1980**, *102*, 3219–3224).

0002-7863/81/1503-7794$01.25/0

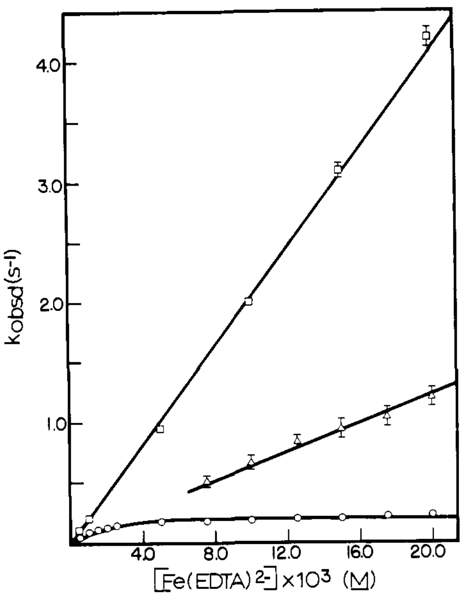

**Figure 1.** Dependences of the observed rate constants on $Fe(EDTA)^{2-}$ concentration for the reduction of ferricytochrome $cd_1$ [25 °C; pH 7.0, $\mu = 0.50$ M (sodium phosphate)]: (□) heme $c$ (550 nm); (△) heme $d_1$ (670 nm), fast phase; (○) heme $d_1$ (670 nm), slow phase.

The kinetic results have been analyzed according to the following mechanism:

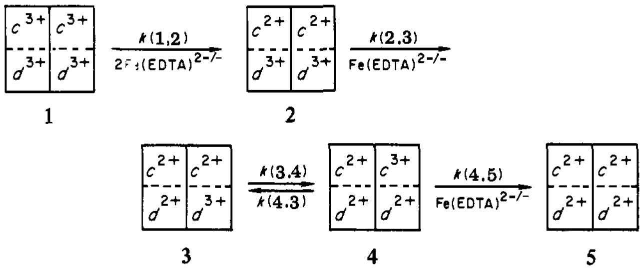

Our data require that **4** be treated as a steady-state intermediate, because **1** → **2** accounts for the observed kinetics of reduction of the heme $c$ groups. The second-order rate constant $k(\mathbf{2,3})$ is obtained from the fast phase of heme $d_1$ reduction, whereas $k(\mathbf{3,4})$ is the limiting rate of the slow phase. The consecutive nature of mechanism **1** → **5** accounts for the induction periods observed in the heme $d_1$ reduction.[8] Values for $k(\mathbf{1,2})$, $k(\mathbf{2,3})$, and $k(\mathbf{3,4})$ obtained from experiments at several different ionic strengths are set out in Table I.

The value of k(**1,2**) is relatively small in comparison with the rate constant[9] for $Fe(EDTA)^{2-}$ reduction of the heme $c$ group in horse heart ferricytochrome $c$ [$k = 2.57 \times 10^4$ $M^{-1}$ $s^{-1}$ (25 °C); $\mu = 0.1$ M) or *Pseudomonas aeruginosa* ferricytochrome $c_{551}$ [$k = 4.2 \times 10^3$ $M^{-1}$ $s^{-1}$ (25 °C); $\mu = 0.1$ M), which is somewhat surprising in view of the fact that the driving force for electron transfer is larger (0.175 vs. 0.140 V) in the case of $cd_1$. Because our studies of the temperature dependence of the bimolecular reduction of the $c$ components revealed[5] no evidence for dramatic mechanistic changes in the electron-transfer process, it is likely that the $c$ heme in each $cd_1$ subunit is located well below the surface of the protein molecule, thereby forcing electron transfer from $Fe(EDTA)^{2-}$ to take place over a relatively long distance. Analysis of the kinetic data in the framework of our modified Marcus-type model[9] for uniformly nonadiabatic electron transfer yields a site (heme $c$)-to-surface distance of 6.9 Å,[5] which is substantially greater than those calculated[9] for $c_{551}$ (4.0 Å) and the horse heart protein (3.4 Å).

Table I. Rate Constants for the Reduction of Ferricytochrome $cd_1$ by $Fe(EDTA)^{2-}$ at Several Ionic Strengths (25 °C; pH 7.0, Sodium Phosphate)

| | heme $c$ | heme $d_1$ | |
|---|---|---|---|
| $\mu$, M | $k(1,2) \times 10^{-2}$, $M^{-1}$ $s^{-1}$ $(\sigma)^a$ | $k(2,3) \times 10^{-2}$ $M^{-1}$ $s^{-1}$ $(\sigma)^b$ | $k(3,4)$, $s^{-1}$ $(\sigma)^c$ |
| 0.05 | 1.72 (2) | | 0.25 (3) |
| 0.10 | 1.91 (15) | | 0.37 (6) |
| 0.20 | 1.86 (6) | | 0.35 (2) |
| 0.30 | 1.90 (3) | 1.04 (7) | 0.31 (1) |
| 0.50 | 1.98 (9) | 0.607 (2.6) | 0.22 (1) |

[a] Standard error of the mean of two or three separate determinations of $k(1,2)$. [b] Standard deviation of the slope as given by a weighted least-squares analysis. [c] Standard deviation of the intercept of the double reciprocal plot as given by a weighted least-squares analysis.

Direct electron transfer from $Fe(EDTA)^{2-}$ to a $d_1$ heme in **1** is very slow relative to the rate of heme $c$ reduction. Once the heme $c$ groups have been reduced, however, bimolecular electron transfer to one of the $d_1$ hemes occurs at an observable rate. After one $d_1$ is reduced (intermediate **3**), the second apparently is not nearly as accessible to external reductants. Full reduction of the $d_1$ sites, therefore, is controlled by the intramolecular electron-transfer step.[10]

Our results thus far show that cytochrome $cd_1$ is a good system to study the kinetic aspects of site–site interactive components in multielectron-transfer reactions. The bimolecular/intramolecular switching mechanism we have discovered for $d_1$ reduction may have important implications for the catalytic chemistry of the enzyme, particularly in regards the binding and electron-transfer steps required for the activation and reduction of substrate oxidants such as $NO_2^-$ and $O_2$. In this context the precise description of the intramolecular electron-transfer step takes on added importance. The key question is whether the $c \rightarrow d_1$ transfer occurs by electron tunneling over a relatively long distance[11] or whether large conformational changes are involved. We hope to shed some light on this matter by measuring and analyzing the temperature dependence of $k(\mathbf{3,4})$; these and related results that bear on the intramolecular electron-transfer mechanism will be reported subsequently.

**Acknowledgment.** We thank Drs. T. E. Meyer and M. D. Kamen for assistance with aspects of enzyme purification. Discussions with Drs. J. J. Hopfield, E. Landaw, R. A. Marcus, D. Pollard, V. T. Taniguchi, and H. E. Toma are acknowledged. This research was supported by National Science Foundation Grant CHE80-24863. S.A.S. was also supported by National Institutes of Health Training Grant 1-T32 HD-07009 (Department of Biophysics and Theoretical Biology, University of Chicago).

---

(8) Computer simulations of the reaction kinetics based on scheme **1** → **5** are in good quantitative agreement with the experimental results at high $Fe(EDTA)^{2-}$ concentrations.[5] Our work on these and related computer simulations indicates that **1** → **5** is the simplest mechanistic scheme that provides an adequate description of the reaction kinetics over a wide range of [$Fe(EDTA)^{2-}$]; at low [$Fe(EDTA)^{2-}$], however, the overall kinetics are simulated better by an extended version of **1** → **5** that includes $c \rightarrow d_1$ transfer in **2** as a parallel pathway. A subsequent paper will deal with the simulations based on **1** → **5** and related mechanisms.

(9) Mauk, A. G.; Scott, R. A.; Gray, H. B. *J. Am. Chem. Soc.* **1980**, *102*, 4360–4363.

(10) Two independent lines of evidence show that intramolecular electron transfer is responsible for the rate saturation observed in the $Fe(EDTA)^{2-}$ reaction: (1) the limiting rate is virtually the same (0.25 $s^{-1}$) for heme $d_1$ reduction by copper(I) azurin under similar conditions of pH, ionic strength, and temperature (Parr, S. R.; Barber, D.; Greenwood, C.; Brunori, M. *Biochem. J.* **1977**, *167*, 447–445); (2) the ionic strength of the medium has little if any influence on the slow phase of the reaction [k(**3,4**), Table I], a finding that rules against any role for a ferricytochrome $cd_1/Fe(EDTA)^{2-}$ precursor complex in the electron-transfer mechanism.

(11) Preliminary calculations based on k(**3,4**) give 13–15 Å for the closest heme $c$ to heme $d_1$ distance.[5]